

Characterization of Alzheimer's disease using EEG as a potential early diagnostic tool

M. Jaico^{1,2}, A. Woll^{1,2}, G. Armoa^{1,2}, S. Herrera^{1,2}

1. Facultad de Ciencias e Ingeniería, Universidad Peruana Cayetano Heredia, Lima, Perú
2. Facultad de Ciencias e Ingeniería, Pontificia Universidad Católica del Perú, Lima, Perú
maria.jaico@upch.pe, alberto.woll@upch.pe, guillermo.armoa@upch.pe, sergio.herrera@upch.pe

Abstract—Alzheimer's disease (AD) is characterized by distinctive cytological, histological, and immunohistochemical changes that differentiate it from normal aging patterns. Although definitive diagnostic confirmation is anatomopathological, current diagnostic criteria combine clinical and biological evidence to formulate a probabilistic diagnosis. Given the high prevalence and socioeconomic impact of AD, there is an intensified search for early diagnostic tools. Electroencephalography (EEG) has emerged as a potential tool for early AD characterization and diagnosis, providing records of brain electrical activity that may reveal specific patterns of neuronal alteration associated with AD before clinical symptoms are evident. This study proposes using EEG to identify spectral power and complexity features to distinguish between healthy individuals and those with AD. The findings suggest that individuals with AD exhibit notable decreases in alpha (8-13 Hz) and beta (13-30 Hz) oscillations compared to healthy controls, which are associated with neuronal deterioration and loss of synaptic connectivity, hallmark characteristics of AD progression.

Keywords —EEG, Alzheimer disease (AD), relative power band (RPB), diagnostic tool, characterization.

I. INTRODUCTION

The Alzheimer's disease (AD) is characterized as a dementia with distinctive cytological, histological, and immunohistochemical changes that differentiate it from patterns of normal aging [1]. While definitive diagnostic certainty of AD is achieved through anatomopathological confirmation, current diagnostic criteria combine clinical and biological evidence to formulate a probabilistic diagnosis. This combination is based on the identification of intraneuronal neurofibrillary tangles, extracellular neuritic plaques, synaptic loss, and other characteristic neuronal changes [1].

Given the high prevalence of AD and its socioeconomic impact, the search for early diagnostic tools has intensified. Among these, the use of electroencephalography (EEG) has emerged as a potential tool for the characterization and early diagnosis of AD. EEG, by providing a record of brain electrical activity, can reveal specific patterns of neuronal alteration associated with AD before clinical symptoms

become evident. This early detection capability is crucial for more effective and timely interventions, which could significantly improve patients' quality of life and reduce the socioeconomic impact of the disease [1].

II. PROBLEM STATEMENT

Neurodegenerative diseases have increased in prevalence over recent years [2]. Currently, 50 million people are affected by these diseases, and this number is projected to exceed 100 million by 2050 [3]. Alzheimer's disease (AD) is a neurodegenerative condition that ranks as the leading cause of dementia worldwide, with early diagnosis posing a significant challenge [4].

Current diagnostic methods include clinical evaluations, neuropsychological tests, cerebrospinal fluid (CSF) biomarkers, and positron emission tomography (PET). These methods can be invasive, costly, and not always readily accessible. Moreover, they often fail to detect the disease until neurological damage is significant [5].

Electroencephalography (EEG) has emerged as a potential alternative tool for AD diagnosis. Several studies have identified specific brain activity patterns that distinguish individuals with Alzheimer's from healthy controls [6], with decreases in alpha and beta oscillations being characteristic features associated with Alzheimer's progression [6]. Furthermore, analysis of brain connectivity via EEG indicates that alterations in connectivity serve as an early marker of AD [7].

Early detection of Alzheimer's disease remains challenging due to its gradual and progressive nature; however, it also presents an opportunity, as current treatments are more effective when administered in the disease's early stages.

III. PROPOSED SOLUTION

The proposed solution involves using EEG for early Alzheimer's diagnosis by identifying power spectrum and complexity characteristics. Additionally, it aims to identify the most representative channels that exhibit significant differences in these characteristics between Alzheimer's patients and healthy individuals.

IV. METHODOLOGY

The methodology used in the study is explained in the diagram in Figure 1.

A. Acquisition of EEG Signals

Figure 2 illustrates the acquisition of signals. The control group comprised 4 male university students aged 20 to 23 from Universidad Peruana Cayetano Heredia. They underwent resting state tests with eyes closed (EC) and eyes open (EO), as well as arithmetic exercises with eyes closed (MAEC) and eyes open (MAEO), each lasting 5 minutes per sample [8]. For the Alzheimer's group, data from the Open Neuro database containing 36 signals from individuals diagnosed with AD was utilized [9].

The Ultracortex Mark IV system was used for signal acquisition, employing the international 10-20 system for electrode placement with 16 channels, following recommendations from the International Federation of Clinical Neurophysiology (IFCN). Electrodes were positioned with reference to the nasion (indentation between the forehead and the upper part of the nose) and inion (palpable prominence in the middle occipital region) [10].

To assess cognitive function in the control group, the Mini-Mental State Examination (MMSE) protocol was employed. This practical tool evaluates cognitive status with scores ranging from 0 to 30, where lower scores indicate severe cognitive impairment [11]. The protocol includes questions related to orientation, registration, attention and calculation, recall, language, and complex commands with eyes closed.

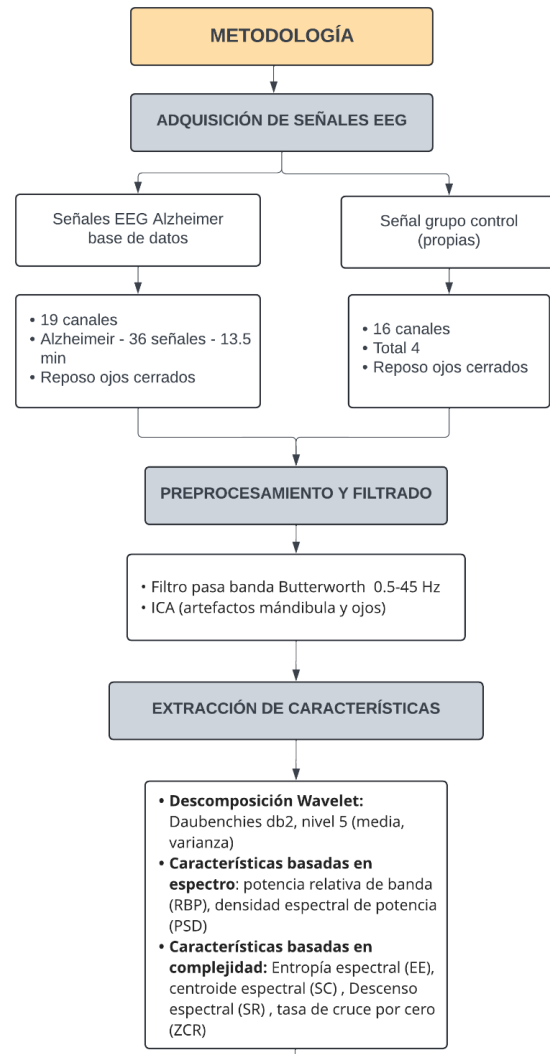


Figure 1. Methodology Flow Diagram



Figure 2. Experimental Setup for EEG Signal Acquisition

B. Preprocessing and Filtering

To compare the signals obtained from the Ultracortex Mark IV with the database signals, we trimmed the database signals to 5 minutes for both groups: the Alzheimer's group and the

control group, whose original durations were 13.5 and 12 minutes, respectively. Additionally, we performed an upsampling process on our Ultracortex Mark IV signals, increasing the sampling frequency from 125 Hz to 500 Hz to match the sampling frequency of the database signals, which was 500 Hz. The signals from the control subjects underwent the same preprocessing and filtering as the signals from the AD group in the database. A Butterworth band-pass filter from 0.5 to 45 Hz was applied. Furthermore, for filtering, the Independent Component Analysis (ICA) method was employed to transform the 16 EEG signals into 16 ICA components and identify muscle artifacts. To each channel of each EE signal

C. Feature Extraction

For feature extraction, a segmentation process was implemented using 3-second windows. Each resulting segment underwent processing algorithms for feature extraction. The filtered signals were subjected to a Daubechies type 2 wavelet decomposition with 5 levels to obtain the mean and variance of each coefficient. Additionally, frequency bands of delta (0.5 - 4 Hz), theta (4-8 Hz), alpha (8-13 Hz), and beta (13-30 Hz) were obtained. Features based on power spectrum such as power spectral density (PSD) and relative band power (RBP) were extracted from the signals. Moreover, complexity-based features such as spectral entropy (SE), spectral centroid (SC), spectral roll-off (SR), and zero-crossing rate (ZCR) were obtained. It is noteworthy that normalized values were used for the power and complexity-based features, while for statistical features such as the mean and variance of the wavelet coefficients, normalized signal values were used.

D. Statistical Analysis

Statistical analysis of EEG signals between AD patients and healthy controls involved mean, standard deviation, and independent samples t-test to analyze differences. Additionally, averages of relative power and complexity across all patient groups were calculated.

IV. RESULTS

The Independent Component Analysis (ICA) allowed for proper filtering by separating EEG signals into independent components and artifacts. For artifact identification, attention was paid to a positive spectral slope between 7 - 75 Hz, characteristic of muscle-origin ICA, and in the topographic map, peripheral foci away from the vertex and a single focal

point that evidences low spatial smoothness, unlike neural components that distribute throughout the map. [12] According to the mentioned criteria, ICA1, ICA7, and ICA13 exhibit a single focal point coinciding with peaks of positive slope in the spectral power graph, along with high variance dispersion, thus identified as artifacts.

According to literature, EEG signals from AD patients may present specific patterns indicating the presence of the disease, such as a significant decrease in relative alpha power and an increase in theta power, reduced synchronization in frequency ranges of 0.5 to 25 Hz [13, 14], EEG signal slowing at rest due to observed neuronal loss in the cerebral cortex, reduced complexity [15], decreased neural network connectivity due to reduced synchrony [H], increased local power in low-frequency bands (delta and theta), and decreased local power in high-frequency bands (alpha and beta) [15].

For feature extraction, 16 common channels were considered between both electrode systems for better comparison of control group data acquired with database data, thus excluding data from Fz, Cz, and Pz channels present in control signals from the database.

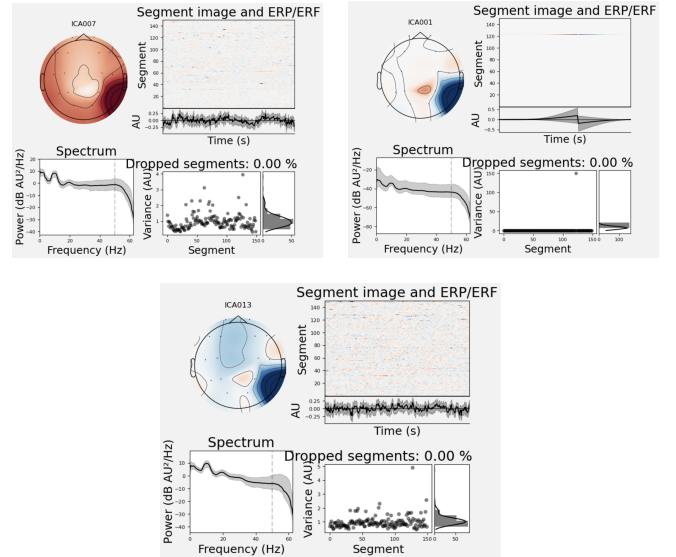


Figure 3. ICA Components 001, 007, and 013

In Figure 7, Relative Band Power (RBP) is presented for control group 1 (own), control group 2 (database), and AD group. The behavior of relative power bands at each frequency reveals a decrease in alpha and beta bands and an increase in delta band values, aligning with the mentioned literature, except for a decrease in theta values.

Additionally, Table I displays complexity-based features such as SE, SC, SR, and ZCR. The zero crossing rate tends to be less complex in individuals with AD, due to the signal not changing its sign from the slowing observed, showing a slight decrease in ZCR value compared to the control group.

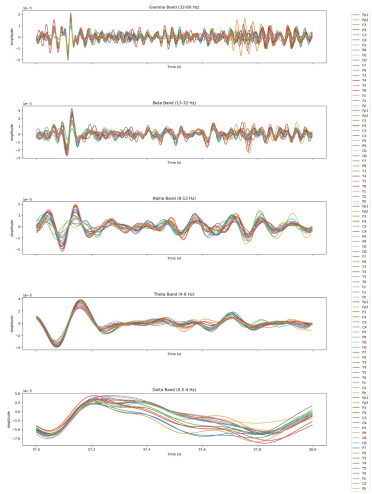


Figure 4. Wavelet Coefficients of Database Control Group

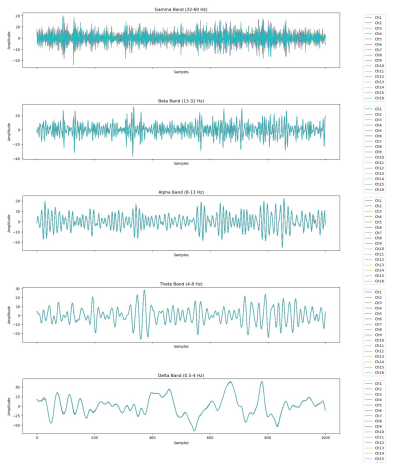


Figure 5. Wavelet Coefficients of Control Group using Ultracortex Mark IV

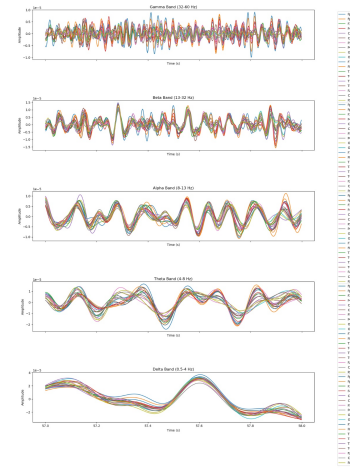


Figure 6. Wavelet Coefficients of Alzheimer's Database Group

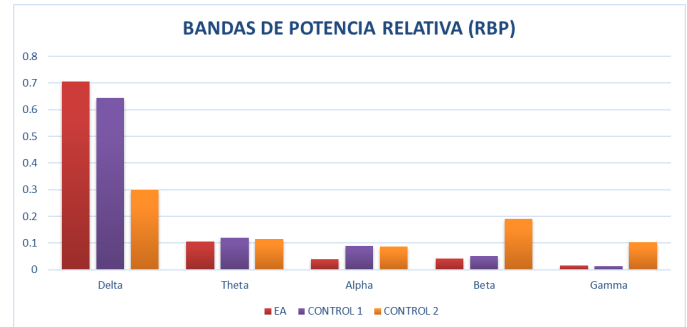


Figure 7. Relative Band Power (RBP) among Alzheimer's group, database control group, and Ultracortex Mark IV control group

Table I
Complexity characteristics

SEÑAL EEG	ENTROPÍA ESPECTRAL	CENTROIDE ESPECTRAL	ROLLOFF ESPECTRAL	TASA DE CRUCE POR CERO
EA	0.551	4.301	212.500	0.015
CONTROL 1	0.567	4.810	212.500	0.016

The parametric t-test was used to determine if relative band power values differ significantly between the control group and Alzheimer's disease group. Table VI shows $p < 0.05$, indicating a significant difference in Beta band relative power between both groups.

Table II
Mean, standard deviation, and percentiles of RBP values in control group (1) and AD group (2)

group	Mean	SD	p25	p50	p75
1	.3429094	.0318876	.3205713	.3514209	.3652476
	.0597316	.0131265	.0505529	.0563371	.0689104
	.0440644	.0202678	.0299303	.0390499	.0581986
	.0430594	.0032517	.0408213	.043722	.0452975
	.0112346	.0021262	.009892	.0111492	.0125773
2	.3753237	.0133479	.3660458	.3784619	.3846016
	.052457	.0089922	.0464106	.0511377	.0585034
	.0196336	.0063115	.015244	.0181365	.0240233
	.0354957	.0040855	.0326639	.0364168	.0383276
	.0144493	.0044825	.0112809	.0129386	.0176178
Total	.3591166	.0285014	.3498387	.3652476	.3784619
	.0560943	.0111184	.0489909	.0526998	.0621407
	.031849	.0190697	.0181365	.027119	.0390499
	.0392775	.0052944	.0364168	.0389502	.043722
	.012842	.0036744	.0110989	.0113313	.0141846

Table III

t-test for Delta Band (RBP) in control group (1) and AD group (2)

.ttest DELTA, by(group) unequal

Two-sample t test with unequal variances

Group	Obs	Mean	Std. err.	Std. dev.	[95% conf. interval]
1	4	.3429094	.0159438	.0318876	.2921692 .3936497
2	4	.3753237	.0066739	.0133479	.3540843 .3965632
Combined	8	.3591166	.0100768	.0285014	.3352888 .3829444
diff	-0.324143	.0172843		-.0803091	.0154805

diff = mean(1) - mean(2)
H0: diff = 0
Ha: diff < 0
Pr(T < t) = 0.0668
Ha: diff != 0
Pr(|T| > |t|) = 0.1336
Ha: diff > 0
Pr(T > t) = 0.9332

Table VI

t-test for Theta Band (RBP) in control group (1) and AD group (2)

.ttest THETA, by(group) unequal

Two-sample t test with unequal variances

Group	Obs	Mean	Std. err.	Std. dev.	[95% conf. interval]
1	4	.0597316	.0065633	.0131265	.0388444 .0806188
2	4	.052457	.0044961	.0089922	.0381484 .0667656
Combined	8	.0560943	.003931	.0111184	.0467991 .0653896
diff	.0072747	.0079556		-.0128245	.0273738

diff = mean(1) - mean(2)
H0: diff = 0
Ha: diff < 0
Pr(T < t) = 0.7999
Ha: diff != 0
Pr(|T| > |t|) = 0.4001
Ha: diff > 0
Pr(T > t) = 0.2001

Table V

t-test for Alpha Band (RBP) in control group (1) and AD group (2)

.ttest ALPHA, by(group) unequal

Two-sample t test with unequal variances

Group	Obs	Mean	Std. err.	Std. dev.	[95% conf. interval]
1	4	.0440644	.0101339	.0202678	.0118139 .076315
2	4	.0196336	.0031558	.0063115	.0095906 .0296767
Combined	8	.031849	.0067422	.0190697	.0159063 .0477917
diff		.0244308	.0106139		-.0064669 .0553285

diff = mean(1) - mean(2)
H0: diff = 0
Ha: diff < 0
Pr(T < t) = 0.9547
Ha: diff != 0
Pr(|T| > |t|) = 0.0906
Ha: diff > 0
Pr(T > t) = 0.0453

Table VI

t-test for Beta Band (RBP) in control group (1) and AD group (2)

.ttest BETA, by(group) unequal

Two-sample t test with unequal variances

Group	Obs	Mean	Std. err.	Std. dev.	[95% conf. interval]
1	4	.0430594	.0016259	.0032517	.0378852 .0482336
2	4	.0354957	.0020428	.0040855	.0289947 .0419967
Combined	8	.0392775	.0018718	.0052944	.0348513 .0437038
diff		.0075636	.0026108		.0010964 .0140309

diff = mean(1) - mean(2)
H0: diff = 0
Ha: diff < 0
Pr(T < t) = 0.9855
Ha: diff != 0
Pr(|T| > |t|) = 0.0290
Ha: diff > 0
Pr(T > t) = 0.0145

Table VII

t-test for Alpha Band (RBP) in control group (1) and AD group (2)

.ttest GAMMA, by(group) unequal

Two-sample t test with unequal variances

Group	Obs	Mean	Std. err.	Std. dev.	[95% conf. interval]
1	4	.0112346	.0010631	.0021262	.0078513 .014618
2	4	.0144493	.0022412	.0044825	.0073167 .0215819
Combined	8	.012842	.0012991	.0036744	.0097701 .0159139
diff		-.0032147	.0024806		-.009925 .0034956

diff = mean(1) - mean(2)
H0: diff = 0
Ha: diff < 0
Pr(T < t) = 0.1302
Ha: diff != 0
Pr(|T| > |t|) = 0.2604
Ha: diff > 0
Pr(T > t) = 0.8698

V. CONCLUSION

The EEG signal of AD patients was characterized by a decrease in ZCR and a notable reduction in alpha (8-13 Hz) and beta (13-30 Hz) oscillations compared to healthy controls; with only the beta oscillations showing a statistically significant difference between groups. These reductions are associated with neuronal deterioration and the loss of synaptic connectivity, which are typical characteristics of the progression of AD.

Additionally, an increase in low-frequency activity, typical of sleep or drowsiness states, was observed. This reflects the loss

of neurons and dysfunction in their connections, particularly in critical areas such as the hippocampus and temporal cortex. The decrease in high-frequency activity, associated with wakefulness, attention, and cognition, could indicate a reduced cerebral capacity to process information, concentrate, and perform complex mental tasks.

For future studies, it is recommended to validate the identified characteristics with a larger study employing patients within the same age range and applying the same protocol to both groups to obtain more comparable results. Moreover, it is crucial to consider the initial damage to the hippocampus and entorhinal cortex, critical structures for the formation of new memories and spatial memory, which are among the first to be affected in AD.

Finally, our long-term goal is to improve analysis and feature extraction algorithms, as well as to identify the channels that show significant differences in these characteristics for each group (AD/healthy). This will enable us to simplify the electrode array for EEG signal acquisition and propose a reduced and innovative design for timely and easy diagnosis.

REFERENCES

- [1] R. F. Allegri et al., "Enfermedad de Alzheimer. Guía de práctica clínica," Neurología Argentina, vol. 3, no. 2, pp. 120–137, Apr. 2011, doi: 10.1016/s1853-0028(11)70026-x.
- [2] 2023 Alzheimer's disease facts and figures. *Alzheimers Dement.* 2023, 19, 1598–1695. <https://pubmed.ncbi.nlm.nih.gov/36918389/>
- [3] World Health Organization . Geneva, Switzerland: World Health Organization; 2021. Fact sheets of dementia [Internet] [cited 2022 Apr 13]. Available from: <https://www.who.int/news-room/fact-sheets/detail/dementia>.
- [4] Rasmussen, J., & Langerman, H. (2019). Alzheimer's Disease – Why We Need Early Diagnosis. *Degenerative Neurological and Neuromuscular Disease*, 9, 123–130. <https://doi.org/10.2147/DNND.S228939>.
- [5] X. Zheng, B. Wang, H. Liu, W. Wu, J. Sun, W. Fang, R. Jiang, Y. Hu, C. Jin, X. Wei, and S. S. Chen, "Diagnosis of Alzheimer's disease via resting-state EEG: integration of spectrum, complexity, and synchronization signal features," *Frontiers in Aging Neuroscience*, vol. 15, 2023. [Online]. Available: <https://www.frontiersin.org/journals/aging-neuroscience/article/s/10.3389/fnagi.2023.1288295>. DOI: 10.3389/fnagi.2023.1288295.
- [6] K. Kudo, K. G. Ranasinghe, H. Morise, F. Syed, K. Sekihara, K. P. Rankin, B. L. Miller, J. H. Kramer, G. D. Rabinovici, K. Vossel, H. E. Kirsch, and S. S. Nagarajan, "Neurophysiological trajectories in Alzheimer's disease progression," *bioRxiv* [Preprint], Mar. 8, 2024. doi: 10.1101/2023.05.18.541379. Update in: *Elife*, vol. 12, Mar. 28, 2024. doi: 10.7554/eLife.91044. PMID: 37293044; PMCID: PMC10245777.
- [7] M. Daianu, N. Jahanshad, T. M. Nir, A. W. Toga, C. R. Jack Jr, M. W. Weiner, and P. M. Thompson, "Breakdown of brain connectivity between normal aging and Alzheimer's disease: a structural k-core network analysis," *Brain Connect.*, vol. 3, no. 4, pp. 407-422, 2013. doi: 10.1089/brain.2012.0137. PMID: 23701292; PMCID: PMC3749712.
- [8] T. N. John, S. D. Puthankattil, and R. Menon, "Analysis of long range dependence in the EEG signals of Alzheimer patients," *Cognitive Neurodynamics*, vol. 12, no. 2, pp. 183–199, Jan. 2018, doi: 10.1007/s11571-017-9467-8.
- [9] Andreas Miltiadous and Katerina D. Tzimourta and Theodora Afrantou and Panagiotis Ioannidis and Nikolaos Grigoriadis and Dimitrios G. Tsalikakis and Pantelis Angelidis and Markos G. Tsipouras and Evripidis Glavas and Nikolaos Giannakeas and Alexandros T. Tzallas (2024). A dataset of EEG recordings from: Alzheimer's disease, Frontotemporal dementia and Healthy subjects. OpenNeuro. [Dataset] doi: doi:10.18112/openneuro.ds004504.v1.0.7
- [10] Unidad de Atención Integral Especializada, "Guía de Procedimiento de Electroencefalografía y Videoelectroencefalografía", Gob.pe. Consultado: 19 de mayo de 2024. [En línea]. Disponible en: [Guía de Procedimiento EEG y VideoEEG](<https://www.insnsb.gob.pe/docs-trans/resoluciones/archivopdf.php?pdf=2022/RD%20N%C2%B0%20000064-2022-DG-INSNSB%20G%20P%20EEG%20Y%20VEEG.pdf>).
- [11] Folstein MF, Folstein SE, McHugh PR. "Mini-mental state". A practical method for grading the cognitive state of patients for the clinician. *J Psychiatr Res.* 1975;12(3):189–198. doi: 10.1016/0022-3956(75)90026-6.
- [12] D. Dharmaprani, H. K. Nguyen, T. W. Lewis, D. DeLosAngeles, J. O. Willoughby and K. J. Pope, "A comparison of independent component analysis algorithms and measures to discriminate between EEG and artifact components," *2016 38th Annual International Conference of the IEEE Engineering in Medicine and Biology Society (EMBC)*, Orlando, FL, USA, 2016, pp. 825-828, doi: 10.1109/EMBC.2016.7590828.
- [13] B. Czigler et al., "EEG cuantitativo en pacientes con enfermedad de Alzheimer precoz. Espectro de potencia y características de complejidad - ScienceDirect," 2008 [Online]. Available: <https://www.sciencedirect.com/science/article/abs/pii/S0167876007002474?via%3Dihub>. [Accessed: 18-May-2024]
- [14] X. Zheng et al., "Diagnosis of Alzheimer's disease via resting-state EEG: integration of spectrum, complexity, and synchronization signal features," vol. 15, p. 1288295, 2023, doi: 10.3389/fnagi.2023.1288295. [Online]. Available:

<https://pubmed.ncbi.nlm.nih.gov/38020761/>. [Accessed: 18-May-2024]

[15] E. Perez-Valero, C. Morillas, M. A. Lopez-Gordo, and J. Mingallon, “Supporting the Detection of Early Alzheimer’s Disease with a Four-Channel EEG Analysis,” vol. 33, no. 4, p. 2350021, Apr. 2023, doi: 10.1142/S0129065723500211.



Jaico Roman Maria José

Seventh-semester student of Biomedical Engineering, interested in the fields of Tissue Engineering and Biomaterials, biotechnology, molecular and synthetic biology.

(maria.jaico@upch.pe)



Armoa Britez Guillermo Javier

Seventh-cycle Biomedical Engineering student, interested in the fields of Biology, Molecular Biology, Tissue Engineering, Biomaterials, and Electronics.

(guillermo.armoa@upch.pe)



Woll García Alberto Gianfranco

Seventh-cycle Biomedical Engineering student, interested in the fields of Circuit Design, Biotechnology, Molecular Engineering, Image Processing, and Project Management.

(alberto.woll@upch.pe)

Herrera del Carpio Sergio Jesús Miguel

Seventh-cycle Biomedical Engineering student, interested in the fields of Medical Signals and Imaging, Electronics, Tissue Engineering, and Biomechanics.

(sergio.herrera@upch.pe)

